Journal of Thermal Science Vol.30, No.5 (2021) 1768−1779

https://doi.org/10.1007/s11630-021-1505-5 **Article ID: 1003-2169(2021)05-1768-12**

Combustion Characteristic and Mechanism of a Mixture Working Fluid C_3H_8/CO_2

SHI Weixiu[1], PAN Lisheng[2,3*], JIN Suyi[1], DONG Yuehua[2,3], LI Teng[2*], ZHAO Jing[2], WEI Xiaolin[2,3]

1. Beijing Engineering Research Center of Sustainable Energy and Buildings, Beijing University of Civil Engineering and Architecture, Beijing 100044, China
2. State Key Laboratory of High-temperature Gas Dynamics, Institute of Mechanics, Chinese Academy of Sciences, Beijing 100190, China
3. School of Engineering Sciences, University of Chinese Academy of Sciences, Beijing 100049, China

Abstract: In the CO_2 transcritical power cycle, conventional cooling water can hardly condense subcritical CO_2 because its critical temperature is as low as 30.98°C. In order to avoid this condensing problem, CO_2-based mixtures have been proposed as working fluids for transcritical power cycle. They can raise the critical temperature by mixing a little C_3H_8 as the secondary component to CO_2. However, the flammability of the mixture may limit its application. This article investigated laminar flame speed of C_3H_8/CO_2 which represents the mixture's combustion characteristic by a so-called heat flux method and studied the inhibition mechanism of CO_2 on the combustion based on the Premixed Laminar Flame-Speed Calculation reactor of Chemkin-Pro. The experimental results showed that the laminar flame speed shows a peak value with changing the equivalence ratio and accelerates with raising the mole fraction of the organic gas. Additionally, a slight upwards trend was observed for the corresponding equivalence ratio of the peaks. The flammable range for the equivalence ratio extended with the mole fraction of C_3H_8 increasing. With the mole fraction of C_3H_8 of 0.15, the maximum laminar flame speed was 12.8 cm/s, 31.7% of that of the pure C_3H_8. The flammable range was from 0.41 to 1.33, decreasing by 23.3% compared with that of C_3H_8. A flammable critical mixing ratio was also found as 0.08/0.92 for C_3H_8/CO_2 at the normal condition. By simulating, it was found that the most key free radical and elementary reaction which determine the inhibition of CO_2 on the combustion are OH and $H+O_2=O+OH$, respectively.

Keywords: CO_2-based mixture, flammability, laminar flame speed, flammable critical mixing ratio, transcritical power cycle

1. Introduction

Faced with the consumption of the fossil energy day to day, many researchers pay their attention to technologies for exploiting and recovering low-grade heat source. It can supply new energy and even reduce the environmental pollution if used in recovering waste heat in industry.

Received: Jan 30, 2021 AE: CHEN Zheng Corresponding author: PAN Lisheng; LI Teng E-mail: panlisheng@imech.ac.cn liteng@imech.ac.cn

Nomenclature

a, b, C	coefficient	λ	thermal conductivity/$W \cdot m^{-1} \cdot °C^{-1}$
D	diameter of premixed gas pipe/cm	ϕ	equivalence ratio
d	thickness of the perforated plate/m	**Subscript**	
q	net heat flux/$J \cdot m^{-1} \cdot s^{-1}$	br	brass
R	radius of perforated plate/m	c	circle center
r	the distance from the measuring points to the center of the perforated plate/m	cr	critical
S	flame combustion rate/$cm \cdot s^{-1}$	L	laminar flow
t	temperature/°C	p	radial direction
U	uncertainty	**Abbreviation**	
$\dot{V}$	volume flow/$L \cdot min^{-1}$	GWP	Global Warming Potential
x	mole fraction	LPG	Liquefied Petroleum Gas
Greek letters		ODP	Ozone Depletion Potential
ε	geometric coefficient of thermal conductivity	ORC	Organic Rankine Cycle

Power cycle using unconventional working fluid has potential to utilize low-temperature heat efficiently to produce power. ORC (Organic Rankine Cycle) and CO_2 power cycles are attracting more and more attention of researchers and companies. Focusing on the expansion process, Pan et al. [1, 2] improved the theoretical method for performance analysis about the power cycle using unconventional working fluid. Long et al. [3] held the point that working fluid with low critical temperature leads to high exergy efficiency as the result of the exergy analysis about the ORC system. It has been proved that the ORC using a mixture working fluid generally gives better performance than that with pure working fluid [4]. Better thermo-economic performance was another important advantage of the mixture working fluid [5]. These are caused by the good glide match of temperature profiles in the evaporator and condenser for the mixture working fluid [6]. Frutiger et al. [7] paid attention to the effect of the uncertainty of fluid properties on ORC performance. In order to predict thermodynamic properties of the mixture fluid accurately, the crossover volume translation SRK (Soave-Redlich-Kwong) equation of state was improved for binary mixtures [8]. Based on a radial flow turbine, Pan et al. [9] executed an experimental study using HCFC123 and HFC245fa as working fluid.

However, some disadvantages limit the application of ORC, such as the high price, the flammability and the harmful effect on the environment [10]. The natural CO_2, in contrast, is cheap, nonflammable, non-toxic and environmentally friendly. Then it is also a very noticeable working fluid for power recovery from low-temperature heat source. Both cycle performance [11] and thermo-economic performance [12] were analyzed using theoretical method. Shu et al. [13] paid attention to managing thermal energy of engine and provided some configurations for CO_2-based transcritical Rankine cycle. Focusing on waste heat, an experimental system was also established successfully for the CO_2 transcritical power cycle and supplied 1.1 kW of a stable power output [14]. However, the conventional cooling water can hardly condense the subcritical CO_2 because of CO_2's low critical temperature, 30.89°C. The application of the CO_2 transcritical power cycle is limited by this condensing problem. Pan et al. [15, 16] proposed and verified a self-condensing CO_2 transcritical power cycle to avoid this problem. Additionally, binary mixture fluids are considered to increase the critical temperature and further make the condensing easier [17]. The organic fluid is a good choice for the second component of the mixture because of its diversity. C_3H_8 is readily available worldwide from Liquefied Petroleum Gas (LPG) [18] and is considered as an alternative refrigerant. Feng et al. [19] pointed out that the mixture working fluid C_3H_8/CO_2 gives a higher relative thermodynamic efficiency comparing with other considered mixtures that consist of hydrocarbon and CO_2. However, a problem of the flammability may be produced by mixing flammable substance into the main component CO_2. Therefore, it is necessary to investigate on the combustion characteristic of the CO_2-based binary mixtures for safe operation. Pan et al. [20] obtained the effect of CO_2 on the combustion characteristic of butane and isobutane and provided the critical flammable mixing ratio for both mixtures. Tian et al. [21] gave the flammability limits of several hydrocarbon/CO_2 mixtures, namely, propance/CO_2, n-butane/CO_2, isobutene/CO_2, n-pentane/CO_2 and isopentane/CO_2. Gant et al. [22] investigated on the flammability of the mixture CH_4/CO_2 and indicated that a stable flame could not be sustained at high CO_2 volume concentration up to around 60% to 70%, but the intermittent flames could still be produced. Cao et al. [23]

also proved that the CO_2 dilution can influence the flame structure as well as the NO formation properties. Tang et al. [24] studied the premixed laminar flame combustion characteristics of C_3H_8 under normal temperature and pressure. Hu et al. [25] provided the results about the laminar flame speed of C_3H_8 under different temperatures and pressures and analyzed effect of the equivalence ratio on the laminar flame speed. C_3H_8 is environment friendly and has already been widely used [26]. This natural environmentally friendly fluid has a zero ODP (Ozone Depression Potential) and a very low GWP (Global Warming Potential). The basic thermodynamic properties of the C_3H_8 and CO_2 are listed in Table 1 [27].

Table 1 Thermodynamic property of the working fluids

Substance	Molar mass/g·mol^{-1}	t_{cr}/°C	p_{cr}/MPa
C_3H_8	44.10	96.74	4.25
CO_2	44.01	30.98	7.38

In order to provide some reference about the flammability of the mixture C_3H_8/CO_2 for the application in not only the power cycle but also the refrigeration cycle, an experimental system was established for measuring laminar flame speed and the combustion characteristic and the critical flammable mixing ratio was obtained. Further, based on the Premixed Laminar Flame-Speed Calculation reactor of Chemkin-Pro, the impact mechanism of CO_2 on the combustion was analyzed.

2. Methodology

2.1 The experimental system and method

In order to reveal the combustion characteristic of the mixture C_3H_8/CO_2, an experimental system was established for measuring the laminar flame speed by a heat flux method. Its schematic diagram can be found in Fig. 1. It mainly consists of a heat flux burner, two thermostatic water baths, three mass flow controllers, an air compressor, a buffer tank, a static mixer and two gas cylinders for CO_2 and C_3H_8. Eight E-type thermocouples are fixed on the perforated plate to measure its temperature distribution. An Agilent data acquisition is used to collect the temperature data. Mass flow rates of the C_3H_8, the CO_2 and the air are controlled and measured by the mass flow controllers and the corresponding software. The two thermostatic water baths supply constant temperature water at 85°C and 25°C, respectively. The details of the burner are shown in Fig. 2. On the perforated plate, the diameter of the small hole is 0.5 mm and the center distance of the holes is 0.7 mm. Since the Seebeck coefficient of E-type thermocouple is larger than that of K-type, T-type and N-type thermocouples, the signal strength is conducive to reducing the noise and error of voltage signal amplification. Therefore, E-type thermocouple was selected for measuring the temperature distribution on the perforated plate. The diameter of a single coupling wire is 0.127 mm and the locations of the thermocouples are shown in Table 2. In order to obtain a thermal insulation for the flat flame which is required by the heat flux method, a stream of hot water is used around the perforated plate of the burner. In a jacket of the burner, a stream of cooling water is used to make temperature of the initial mixed gas from the static mixer keep constant. The buffer tank can stabilize the pressure of the air from the air compressor. In the static mixer, three flows of gas mixed together before the combustion.

In this experimental research, the combustion characteristic of the mixture with different mixing ratios was investigated. The mole ratio or the volume ratio is used in this study. The mole fraction of the C_3H_8 can be expressed as:

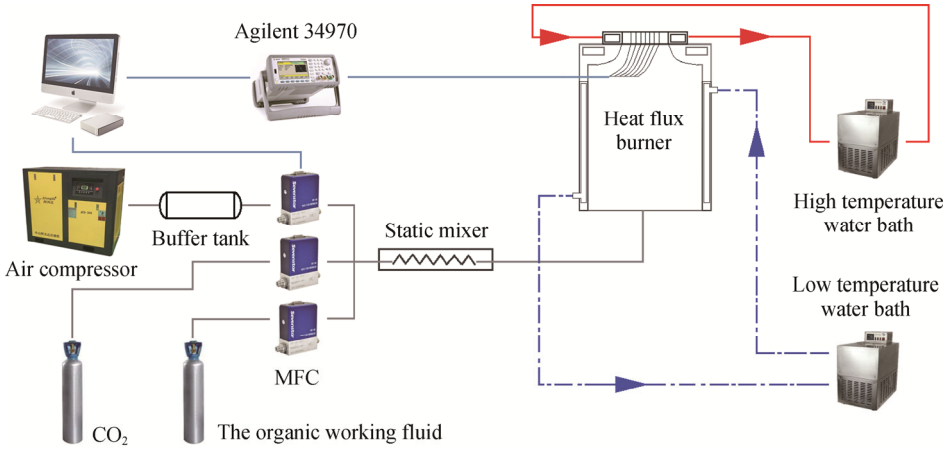

Fig. 1 Schematic diagram for flame speed testing system

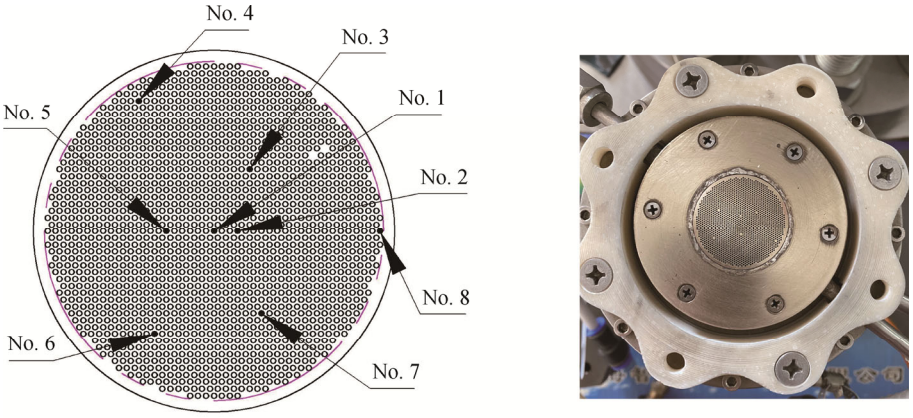

(a) Layout of the perforated plate thermocouple (b) Top view of the heat flux burner

Fig. 2 Burner details

Table 2 Thermocouple measuring point coordinates

Thermocouple number	No. 1	No. 2	No. 3	No. 4	No. 5	No. 6	No. 7	No. 8
Angle to horizontal/(°)	0	0	60	120	180	240	300	360
Distance from the center/mm	0	2.1	6.3	13.3	4.2	10.5	8.4	14.7

$$x_{C_3H_8} = \frac{\dot{V}_{C_3H_8}}{\dot{V}_{CO_2} + \dot{V}_{C_3H_8}} \tag{1}$$

The principle of the heat flux method is that the laminar flame speed is equal to the flow velocity of the premixed gas when the flat flame is in an adiabatic state which can be identified by the uniform of the temperature of the measuring point on the perforated plate surface. Maaren. [28] provided the radial temperature distribution on the perforated plate by analyzing the two-dimensional heat conduction of the perforated plate.

$$\overline{t}_p(r) = -\frac{a}{b} + \left[\frac{q\left(R^2 - r^2\right)}{2db\varepsilon} + \left(\frac{a}{b} + t_R\right)^2\right]^{\frac{1}{2}} \tag{2}$$

The parameter t_R represents the temperature at the edge of the perforated plate.

The thermal conductivity of the perforated plate in the radial direction is calculated according to Eq. (3):

$$\lambda_p = \varepsilon\lambda_{br}\left(t\right) = \varepsilon\left(a + b\cdot t\right) \tag{3}$$

Next, a simplified form of Eq. (2) can be obtained as:

$$\overline{t}_p\left(r\right) = t_c - \frac{q}{4\lambda_p d}r^2 = t_c + Cr^2 \tag{4}$$

where t_c represents the temperature at the center of the perforated plate.

According to the above equation, the flame adiabatic coefficient C can be obtained by fitting method. Using interpolation method, laminar flame speed equals mixed gas flow velocity when C equals 0 under the corresponding equivalence ratio ϕ.

2.2 Uncertainty of the measurement

In this experiment, mass flow rates of the C_3H_8, CO_2 and air were controlled and measured by three flow controllers whose accuracy is ±0.35% of the corresponding full span. Their full span is 6 L/min, 15 L/min and 30 L/min, respectively. Then standard uncertainty of flow velocity for C_3H_8, CO_2 and air is $0.021/\sqrt{3}$ L/min, $0.0525/\sqrt{3}$ L/min and $0.105/\sqrt{3}$ L/min, respectively. The accuracy of the E-type thermocouples is ±0.5°C, so the standard uncertainty of temperature distribution can be obtained as $0.5/\sqrt{3}$ °C.

In this experiment, the equivalence ratio is defined as the quotient of the theoretical air quantity needed and the actual air quantity. The theoretical air quantity needed in the combustion process for one volume C_3H_8 is 23.8 volumes air, if the fuel completely burns out and the oxygen fraction of the air is specified as 0.21. Therefore, the equivalence ratio can be expressed as:

$$\phi = \frac{\dot{V}_{air,need}}{\dot{V}_{air,real}} = \frac{23.8\times\dot{V}_{C_3H_8}}{\dot{V}_{air,real}} \tag{5}$$

It is worth noting that the above equation is also suitable for the combustion of the mixture C_3H_8/CO_2. For equivalence ratio, the uncertainty value is calculated by Eq. (6):

$$U_\phi = \sqrt{\left(U_{\dot{V}_{C_3H_8}}\frac{\partial\phi}{\partial\dot{V}_{C_3H_8}}\right)^2 + \left(U_{\dot{V}_{air}}\frac{\partial\phi}{\partial\dot{V}_{air}}\right)^2} \tag{6}$$

A pipe with its internal diameter of 30 mm is selected for the premixed gas flow, so the laminar flame speed can be calculated according to Eq. (7):

$$S_{\mathrm{L}}=\frac{298\ 150\times\left(\dot{V}_{\mathrm{C_3H_8}}+\dot{V}_{\mathrm{CO_2}}+\dot{V}_{\mathrm{air}}\right)}{0.25\cdot\pi\cdot D^2\times273.15\times60}=2.574\cdot\left(\dot{V}_{\mathrm{C_3H_8}}+\dot{V}_{\mathrm{CO_2}}+\dot{V}_{\mathrm{air}}\right) \tag{7}$$

Consequently, the uncertainty value of laminar flame speed can be expressed as:

$$U_{S_{\mathrm{L}}}=\left[\left(U_{\dot{V}_{\mathrm{C_3H_8}}}\frac{\partial S_{\mathrm{L}}}{\partial\dot{V}_{\mathrm{C_3H_8}}}\right)^2+\left(U_{\dot{V}_{\mathrm{CO_2}}}\frac{\partial S_{\mathrm{L}}}{\partial\dot{V}_{\mathrm{CO_2}}}\right)^2+\left(U_{\dot{V}_{\mathrm{air}}}\frac{\partial S_{\mathrm{L}}}{\partial\dot{V}_{\mathrm{air}}}\right)^2\right]^{\frac{1}{2}} \tag{8}$$

Based on these equations, the uncertainty of the laminar flame speed can be found as 0.16 cm/s for C_3H_8 and 0.18 cm/s for C_3H_8/CO_2. The values are much lower than the corresponding laminar flame speed, so uncertainty of the laminar flame speed is not shown in the following figures. However, it is worth noting that two other factors, accuracy of E-type thermocouples and fitting processes, influence uncertainty of the laminar flame speed. Additionally, the temperature uncertainty can transmit during fitting processes. However, it is very hard to evaluate the fitting uncertainty and the transmission of the temperature uncertainty. Therefore, this study only takes uncertainty of the flow rate meter into account rather than that of thermocouples and fitting processes.

2.3. Simulation method

The Premixed Laminar Flame-Speed Calculation reactor of Chemkin-Pro and the combustion mechanism of USC Mech II [29] were used in the simulation investigation on the inhibition mechanism of CO_2 on the combustion. The combustion mechanism of USC Mech II consists of 111 components and 784 elementary reactions. In a combustion process, the generation and consumption of free radicals is crucial to the combustion characteristic [30]. Therefore, this simulation research focused on looking for the key free radicals and elementary reactions. The key free radicals which impact the laminar flame speed were obtained by the analysis of rate of production (ROP) and the latter was got by sensitivity analysis of the laminar flame speed. In the simulation, the inlet velocity was set as 5.65 cm/s. The operating temperature and pressure were specified as 25°C and 0.1 MPa.

3. Results and Discussion

3.1 Verification of experimental system and combustion mechanism

In order to verify the reliability of the experimental system and the theoretical combustion mechanism, the laminar flame speeds of pure C_3H_8 with different equivalence ratios were obtained by experiments and simulations and were further compared with results measured by various experimental methods, including the heat flux method [31], the constant volume incendiary bomb method [25, 32], the spherical flame method [33], the improvement method of Bunsen burner [34] and the counter flow flame method [35].

The experimental results by the heat flux method and simulation results in this work, together with some data from the references are shown in Fig. 3. Generally speaking, the results obtained agree with the corresponding previous work. The variations of the laminar flame speed with the equivalence ratio are similar and the peaks appear with the equivalent ratio of around 1.1. From the experimental results, in the considered equivalence ratio range from 0.5 to 1.6, the laminar flame speed increases firstly and then decreases with the increase of the equivalence ratio. Then a peak value can be found to be 40.3 cm/s at the equivalence ratio of 1.0. The laminar flame speed got by simulating shows similar variation with equivalence ratio and the maximum value is 40.2 cm/s at the equivalence ratio of 1.1. The above results proved that this experimental system and the selected combustion mechanism are reliable enough. The theoretical flammable range of C_3H_8 can be obtained by fitting the laminar flame speed and extending the fitting line to the axis of the equivalence ratio. The equivalences at the intersections with the laminar flame speed of 0 cm/s are the lower and upper flammable limits. Using this theoretical method, the lower flammable limit can be found to be 0.41 and the upper flammable limit is 1.61.

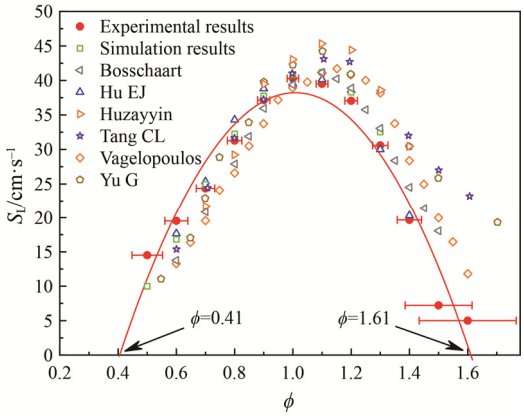

Fig. 3 Variation of laminar flame speed of pure C_3H_8 with the equivalence ratio

3.2 The influence of the equivalence ratio

In the following experiment, the combustion characteristic of the mixture was executed. Firstly,

attention was paid to the influence of the equivalence ratio on the combustion characteristic. Then a mixing ratio of 0.25/0.75 for the mixture C_3H_8/CO_2 was selected for this series of experiments and the considered equivalence ratio varied from 0.5 to 1.3.

As shown in Fig. 4, the laminar flame speed shows a parabola shape as similar as the pure C_3H_8. The watershed locates at approximate 0.9 of the equivalence ratio with the peak value of 20.5 cm/s. The combustion intensity increases with raising the equivalence ratio when it is lower than 0.9. In the other conditions, the laminar flame speed is reduced by decreasing air in the premixed gas. As also indicated in the figure, the flame shape varies with changing equivalence ratio. When the equivalence is 0.5, the flame is slightly lifted by the excess air and it looks like a dish. In the conditions with the equivalence ratio of 0.6, 0.7, 0.8, and 0.9, the flame shows a stable flat flame. Then, with increasing the equivalence ratio continually, a slight cone flame begins to appear and finally it changes into a double-layer flame in the fuel-rich condition. It should be noted that the double-layer flame is already not an exact flat flame. The flame was unstable with equivalence ratio lower than 0.6 and further it burned out with the equivalence ratio of 0.4.

Compared with the maximum laminar flame speed of the pure C_3H_8, the value decreased by 48.5% due to the existence of the large amount of CO_2. The theoretical lower and upper flammable limits of the mixture can also be founded by fitting the experimental results and extending the fitting line. The theoretical lower flammable limit is 0.38 and the upper flammable limit is 1.40. In addition, the CO_2 can inhibit the combustion of C_3H_8 slightly, so the flammable range decreases by 15% and goes to the oxygen-rich side a little compared with the combustion of the pure C_3H_8.

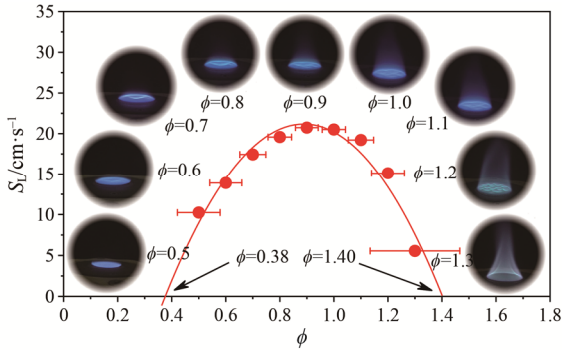

Fig. 4 Variation of the laminar flame speed and the flame shape of the mixture C_3H_8/CO_2 (0.25/0.75) with the equivalence ratio

3.3 The influence of the mixing ratio

This section focuses on the influence of the mixing ratio. The variation of the laminar flame speed was provided for the mixture C_3H_8/CO_2 with the equivalence ratio of 1.0 at different mixing ratio. Furthermore, the detailed laminar flame speed at different equivalence ratio and mixing ratio were obtained and the influence of the mixing ratio was revealed on the flammable range, the peak laminar flame speed and the corresponding equivalence ratio.

As shown in Fig. 5, the laminar flame speed at the equivalence of 1.0 increases approximately straight up with mixing more C_3H_8 into the mixture. It can be found easily that the laminar flame speed of the mixture is much lower than that of the pure C_3H_8 and the difference increases with raising the fraction of the CO_2. The laminar flame speed with the mole fraction of C_3H_8 of 0.15 is 11.8 cm/s, only 28.8% of that of the pure C_3H_8. The reason is that the mixture was diluted with the nonflammable CO_2 and moreover the CO_2 can restrain the combustion reaction.

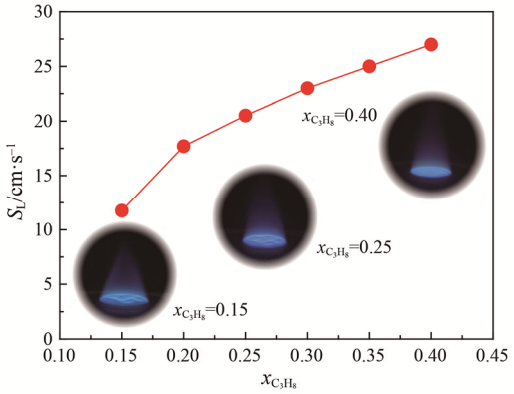

Fig. 5 Variation of laminar flame speed and flame shape of the mixture C_3H_8/CO_2 with the mixing ratio at the equivalence ratio of 1.0

When the mole fraction of the CO_2 is small, the flame is flat and stable. In the other conditions, some small waves appeared on the flat flame and the flame became weak as raising mole fraction of CO_2. Additionally, combustion could only last for a very short time and would soon burn out with the mole fraction of C_3H_8 smaller than 0.15. In other words, the combustion was very unstable and the mixture was almost nonflammable with that mixing ratio. The searching for the flammable critical mixing ratio was carried out in the following section.

Besides the speed, the mixing ratio also includes the flammable range for the equivalence ratio and the according equivalence ratio for the maximum laminar flame speed.

As shown in Fig. 6, the shapes of the curves for the laminar flame speed are similar to each other. The speed including the peak value accelerates with raising mole fraction of C_3H_8. In considered conditions, the peak value with the mole fraction of C_3H_8 of 0.15 is 12.8 cm/s that

was 31.7% of that of the pure organic substance. Though the mixture working fluid becomes flammable with mixing more C_3H_8 into it continually, the existence of a natural combustion inhibitor, the CO_2, can weaken the combustion intensity obviously. Besides the laminar flame speed, it is also indicated that the flammable range for the equivalence ratio extends with the increase of C_3H_8's mole fraction. For example, flammable range for the mixture C_3H_8/CO_2 (0.15/0.85) is from 0.40 to 1.33 while that for the pure C_3H_8 extends to 0.41–1.61. That is to say that the mixture with more C_3H_8 is more flammable. The increase of the flammable range means the weakening of the operating safety. There are minor differences for the lower flammable limits and obvious differences for the upper flammable limits, so the inhibition effect of the CO_2 on the combustion is more obvious in the fuel-rich conditions. There is another statement worth noting that three data points were abandoned because the flame became very unstable rather than a stable flat flame in these three conditions. They show fluctuating flames that were going to be blown out.

The shift of the peak of the laminar flame speed curve with changing the mixing ratio is another interesting phenomenon. As shown in Fig. 6, besides the variation of the maximum speed and the flammable range, the peak point also goes towards right slightly, a direction towards a higher equivalence ratio. The dilution and the inhibition

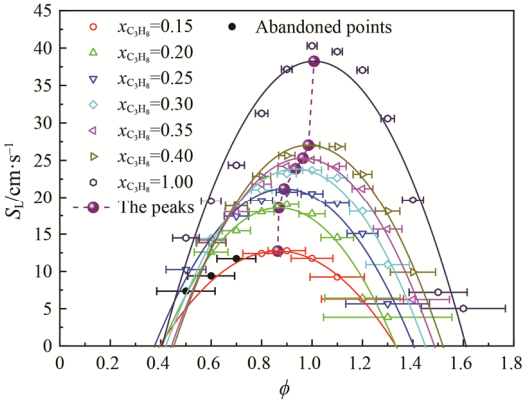

Fig. 6 The detailed combustion characteristic of the mixture C_3H_8/CO_2 with different equivalence ratio and mixing ratio

of the main component, CO_2, are the two fundamental factors that affect the combustion characteristic. The CO_2 absorbs heat in the combustion reaction, which decreases the combustion temperature and the flame speed. These two factors dominate in the fuel-rich conditions in which the relative quantity of the CO_2 compared with air or nitrogen is much larger than that in the oxygen-rich conditions. Therefore, the effect of the CO_2 on the laminar flame speed and the flammable limit is much more obvious in the fuel-rich conditions than that in the oxygen-rich conditions. An obvious increase of the laminar flame speed in the fuel-rich conditions indirectly drives the peak point to move towards higher equivalence ratio.

3.4 The flammable critical mixing ratio

By the above experimental investigation, the detailed combustion characteristic of the mixture working fluid C_3H_8/CO_2 is provided. Researchers and engineers can select the mixing ratio referring to corresponding combustion data. Besides, there is another important parameter named the flammable critical mixing ratio which is helpful for safe operation. It is defined as the mole mixing ratio of the two components of the mixture. If the actual mole fraction of C_3H_8 is less than its flammable critical mole fraction, the mixture is completely nonflammable with any equivalence ratio and a good choice for preventing fire and explosion. In the following comes the result and the discussion about the flammable critical mixing ratio.

When the mole fraction of the C_3H_8 is 0.15, the mixture can generate a stable flat flame in some conditions while the flame in other conditions begins to be very weak and unstable. As decreasing the relative amount of the C_3H_8 continually, the flame was becoming weaker and weaker and burned out finally with the mole fraction down to 0.08. That is to say that flammable critical mixing ratio for the mixture C_3H_8/CO_2 is 0.08/0.92. The flame, not a flat flame already, can exist with the equivalence ratio in the range of 0.5–0.8, which is shown in Fig. 7. When the equivalence ratio is 0.4 or less, the premixed gas kept burning for a very short time and then burned out quickly. On the other hand, the premixed gas can't be ignited with equivalence ratio of

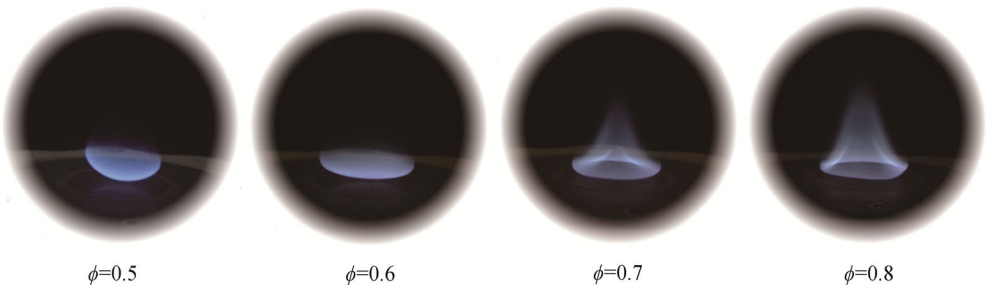

Fig. 7 The flame shape of the mixture C_3H_8/CO_2 (0.08/0.92) at different equivalence ratio

0.8 or larger. With the equivalence of 0.5, the flame was blown off the burner surface by the premixed gas and curled upwards inwardly. Generally, it looks like a hemispherical. Because of the increase of the mixture in the premixed gas, the flame went towards the burner surface slightly in the condition in which the equivalence ratio is 0.6. The flame was shaped like a bowl or a dish. Unlike the other experiment series, the double-layer flame appeared with very low equivalence ratio, 0.7. Although the combustion reaction is still in the oxygen-rich condition, some flammable substance has no chance to meet the oxygen and combustion immediately because of the large amount of CO_2. Then it burns on the second layer of the flame. The height and the bottom area increased with raising the equivalence ratio from 0.7 to 0.8. If the equivalence ratio is raised continually, the flame became unstable with jumping up and down and burned out quickly. The mixture is nonflammable with lower mole fraction of C_3H_8.

However, it should be noted that too low mole fraction of the C_3H_8 harms the enhancement of the critical temperature and the cycle performance. This study provides a reference for specifying the mixing ratio, but the final value should also consider other factors like thermodynamic performance and heat source.

3.5 Impact mechanism of CO_2 on the combustion

3.5.1 Key free radicals

The free radicals, OH, H and O, are very important for the combustion and are potential influencing factors by diluting the fuels [36, 37]. The free radical whose maximum mole fraction is linearly related with the laminar flame speed is the most critical one for influencing the speed in the combustion [38]. The maximum mole fraction of these free radicals and the laminar flame speed are obtained with the mole fraction of C_3H_8 of 0.20, 0.6 and 1.0. The considered equivalence ratio is from 0.5 to 1.3. As shown in Fig. 8, the laminar flame speed generally increases with the increase of the maximum mole fraction of each radical. Further, the maximum mole fraction of OH+H shows the strongest linear correlation with the laminar fame speed, which indicates that the laminar flame speed is closely related to the free radicals OH and H. For a single free radical, OH is the key radial that impacts the laminar flame speed of the combustion. The free radical of H comes the second.

The rate of production (ROP) of OH and H varies with the distance from the considered position to the entrance of the reactor and the mole fraction of C_3H_8 as shown in Fig. 9. Negative value of ROP indicates consumption and positive one represents production of the considered free radical at the position. As shown in the figures, the extreme values appear later and later with increasing the mole fraction of CO_2. In addition, the maximum consumption/production rate decreases with raising the mole fraction of CO_2, and this trend is more obvious with higher fraction of CO_2. That means the impact of CO_2 on the combustion grows with mixing more CO_2 into the fuel.

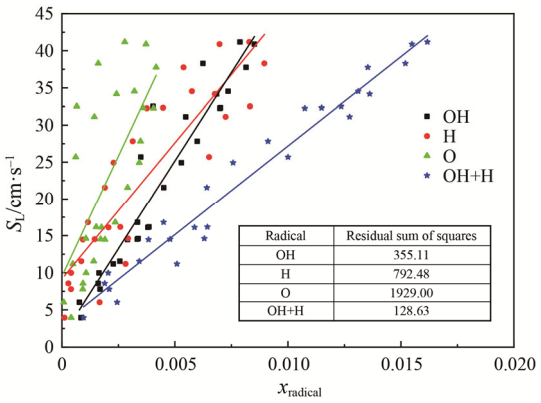

Fig. 8 Linear correlation of the maximum mole fraction of free radicals and laminar flame speed

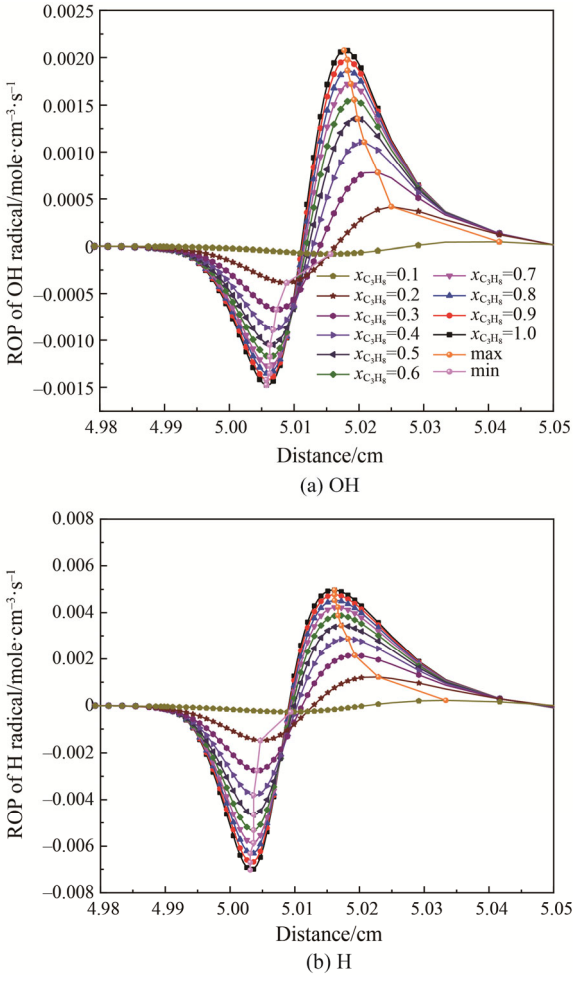

Fig. 9 Variation of ROP of OH and H with the equivalence ratio of 1.0

3.5.2 Key elementary reactions

In different combustion conditions, the rank of key elementary reactions for normalized sensitivity coefficient of laminar flame speed are also different. Table 3 shows the top four key elementary reactions for different mixing ratio conditions with equivalence ratio of 1. These seven reactions (Reaction 1, 9, 12, 31, 35, 88 and 410) are the most dominant key elementary reactions.

Further, the quantitative comparison of these seven key elementary reactions is shown in Fig. 10. The positive sensitivity coefficient represents that the laminar flame speed can be increased by increasing the reaction rate of this elementary reaction and vice versa. Therefore, Reaction 1 and 31 have positive sensitivity coefficient while the other reactions have negative sensitivity coefficient. There is only a little difference of the sensitivity coefficient for the same reaction at different mixing ratios. For all considered mixing ratios, Reaction 1 has the largest sensitivity coefficient among these seven reactions and its value is much higher than the others. That is to say, Reaction 1, $H+O_2=O+OH$, is the most important key elementary reaction which impacts the laminar flame speed.

Table 3 Top key elementary reactions for normalized sensitivity coefficient of laminar flame speed with equivalence ratio of 1.0

Mole fraction of C_3H_8	Key elementary reactions
0.1	Reaction 1>Reaction 9>Reaction 12>Reaction 410
0.2	Reaction 1>Reaction 9 > Reaction 12>Reaction 88
0.3	Reaction 1>Reaction 9>Reaction 35>Reaction 88
0.4	
0.5	Reaction 1>Reaction 9>Reaction 31>Reaction 88
0.6	
0.7	
0.8	Reaction 1>Reaction 9>Reaction 31>Reaction 35
0.9	
1.0	

CO_2 can be regarded as diluent in the combustion process of C_3H_8-air. It impacts the combustion by three effects, namely, dilution effect, thermal effect and chemical effect. With increasing mole fraction of CO_2, the fuel of C_3H_8 is diluted and its concentration decreases. On the other hand, as shown in Fig. 11, the adiabatic flame temperature decreases because of the thermal effect of CO_2, which leads to the decrease of the laminar flame speed [39]. The most interesting thing is that CO_2 directly takes part in this chemical reaction. For example, the inputting CO_2 strengthens the reverse reaction of Reaction 31. It consumes free radical of H in Reaction 31, further competes for H in Reaction 1 which is the most sensitive elementary reaction and thus inhibits the combustion process [37]. The combustion is weakened and more free radical of CO is produced, which inhibits the elementary Reaction 35. In general, for elementary reactions that do not involve in the mutual transformation of OH and H, the sensitivity coefficient is positive in elementary reactions generating free radicals of OH and H and is negative in elementary reactions consuming these two free radicals. This indicates once again that the laminar flame speed is closely related to OH and H radicals. In addition, it is noted that the most key elementary Reaction 1 involves three free radicals that are crucial to combustion, OH, H, and O, respectively.

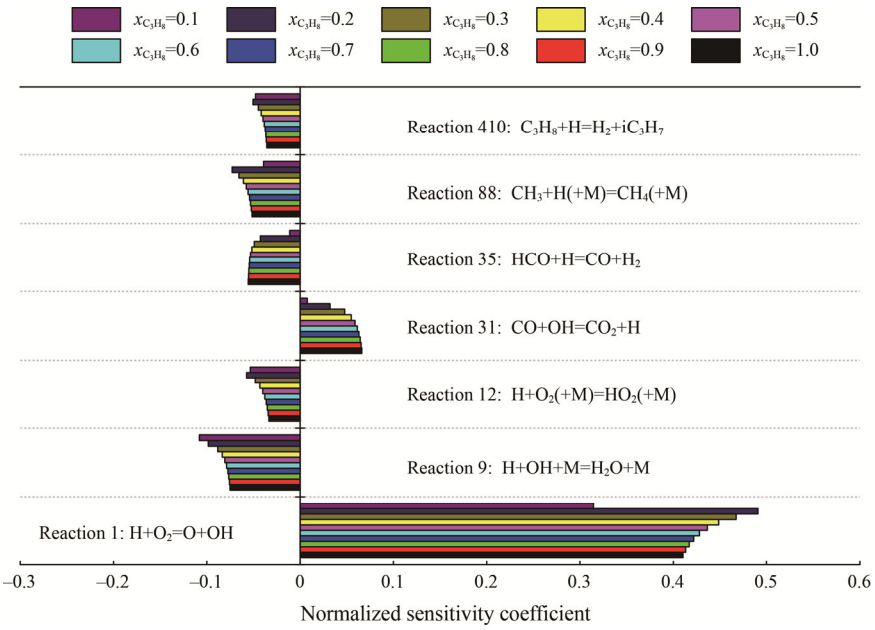

Fig. 10 Normalized sensitivity coefficient of laminar flame speed with equivalence ratio of 1.0

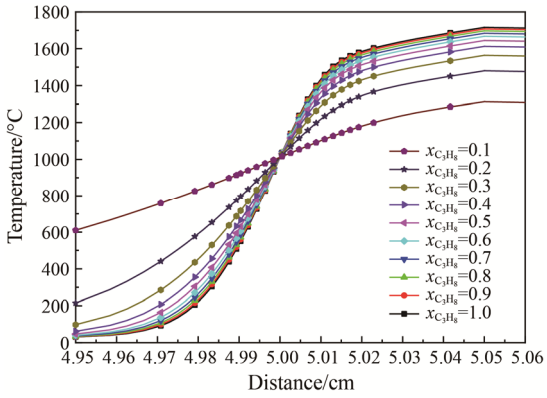

Fig. 11 Variation of adiabatic flame temperature with distance at equivalence ratio of 1.0

4. Conclusions

In order to provide flammability of the mixture working fluid C_3H_8/CO_2 which has potential to realize a transcritical power cycle using conventional cooling water, an experimental system was established for measuring the laminar flame speed using the heat flux method. The combustion characteristic of the mixture as well as the pure C_3H_8 was obtained. The parameters discussed detailedly include the laminar flame speed, the flammable range for the equivalence ratio, the flammable critical mixing ratio and so on.

(1) The laminar flame speed shows a peak value with changing the equivalence ratio and accelerates with raising the mole fraction of the organic gas. Additionally, a slight upwards trend was observed for the corresponding equivalence ratio of the peaks. With the mole fraction of C_3H_8 of 0.15, the maximum laminar flame speed was as low as 12.8 cm/s, 31.7% of that of the pure C_3H_8.

(2) The flammable range for the equivalence ratio extends and the mixture becomes more flammable as raising mole fraction of C_3H_8. With the mole fraction of C_3H_8 of 0.15, the flammable range was from 0.41 to 1.33, being less by 23.3% than that of the pure C_3H_8. The effect of the CO_2 is more obvious on the upper flammable limit than the lower flammable limit. So the flammable range shifted towards fuel-rich field slightly with raising the relative amount of C_3H_8.

(3) The flammable critical mixing ratio was obtained, as 0.08/0.92 for C_3H_8/CO_2 at normal temperature and pressure. The mixture is nonflammable with lower mole fraction of C_3H_8. However, because the mole fraction of the C_3H_8 affects the critical temperature and the cycle performance, other factors like thermodynamic performance and heat source should also be taken into account.

(4) Several flame shapes were observed in the experiment. The flat flame appeared in the conditions when equivalence ratio is around 1.0. The lifted flame, like a bowl, was common in the oxygen-rich field while the double-layer flame usually was in the fuel-rich field.

(5) The key free radicals that affect the laminar flame speed are OH and H. In the combustion process, the maximum mole fraction of OH+H has the strongest linear correlation with the laminar flame speed. The free radical of OH has the closest relationship with the laminar flame speed, followed by the free radical of H. The laminar flame speed is most sensitive to elementary Reaction 1 ($H+O_2=O+OH$) which is the most crucial elementary reaction. Except diluting effect, the inputting CO_2 reduces the concentration of free radical H mainly by elementary Reactions 1 and 31.

Acknowledgments

Projects 51776215 and 51736010 supported by National Natural Science Foundation of China are gratefully acknowledged.

References

[1] Pan L., Wang H., Improved analysis of Organic Rankine Cycle based on radial flow turbine. Applied Thermal Engineering, 2013, 61(2): 606–615.

[2] Pan L., Shi W., Investigation on the pinch point position in heat exchangers. Journal of Thermal Science, 2016, 25(3): 258–265.

[3] Long R., Bao Y., Huang X., Liu W., Exergy analysis and working fluid selection of organic Rankine cycle for low grade waste heat recovery. Energy, 2014, 73: 475–483.

[4] Mahmoudi A., Fazli M., Morad M., A recent review of waste heat recovery by organic Rankine cycle. Applied Thermal Engineering, 2018, 143: 660–675.

[5] Feng Y., Hung T., Greg K., Zhang Y., Li B., Yang J., Thermoeconomic comparison between pure and mixture working fluids of organic Rankine cycles (ORCs) for low temperature waste heat recovery. Energy Conversion and Management, 2015, 106: 859–872.

[6] Heberle F., Preißinger M., Brüggemann D., Zeotropic mixtures as working fluids in organic Rankine cycles for low-enthalpy geothermal resources. Renewable Energy, 2012, 37: 364–370.

[7] Frutiger J., Andreasen J., Liu W., Spliethoff H., Haglind F., Abildskov J., Sin G., Working fluid selection for organic Rankine cycles – impact of uncertainty of fluid properties. Energy, 2016, 109: 987–997.

[8] Shen A., Liu Q., Duan Y., Yang Z., Crossover VTSRK equation of state for selected alkane + alkane and CO_2 + alkane binary mixtures. Fluid Phase Equilibria, 2016, 408: 180–189.

[9] Pan L., Wang H., Experimental investigation on

performance of an organic Rankine cycle system integrated with a radial flow turbine. Energies, 2019, 12(4): 724.

[10] Wu C., Yan X., Wang S., Bai K., Di J., Cheng S., Li J., System optimisation and performance analysis of CO_2 transcritical power cycle for waste heat recovery. Energy, 2016, 100: 391–400.

[11] Kim Y., Kim C., Favrat D., Transcritical or supercritical CO_2 cycles using both low- and high-temperature heat sources. Energy, 2012, 43: 402–415.

[12] Li M., Wang J., Li S., Wang X., He W., Dai Y., Thermo-economic analysis and comparison of a CO_2 transcritical power cycle and an organic Rankine cycle. Geothermics, 2014, 50: 101–111.

[13] Shu G., Shi L., Tian H., Deng S., Li X., Chang L., Configurations selection maps of CO_2-based transcritical Rankine cycle (CTRC) for thermal energy management of engine waste heat. Applied Energy, 2017, 186: 423–435.

[14] Pan L., Wei X., Li B., Li T., Experimental investigation on the CO_2 transcritical power cycle. Energy, 2016, 95: 247–254.

[15] Pan L., Li B., Shi W., Wei X., Optimization of the self-condensation CO_2 transcritical power cycle using solar thermal energy. Applied Energy, 2019, 253: 113608.

[16] Pan L., Shi W., Wei X., Li T., Li B., Experimental verification of the self-condensing CO_2 transcritical power cycle. Energy, 2020, 198: 117335.

[17] Pan L., Wei X., Shi W., Performance analysis of a zeotropic mixture (R290/CO_2) for trans-critical power cycle. Chinese Journal of Chemical Engineering, 2015, 23: 572–577.

[18] Yelishala S.C., Wang Z., Metghalchi H., Levendis Y.A., Kannaiyan K., Sadr R., Effect of carbon dioxide on the laminar burning speed of propane-air mixtures. Journal of Energy Resources Technology, 2019, 141(8): 082205.

[19] Feng L., Zheng D., Chen J., Dai X., Shi L., Exploration and analysis of CO_2 + hydrocarbons mixtures as working fluids for trans-critical ORC. Energy Procedia, 2017, 129: 145–151.

[20] Pan L., Ma Y., Li T., Li H., Li B., Wei X., Investigation on the cycle performance and the combustion characteristic of two CO_2-based binary mixtures for the transcritical power cycle. Energy, 2019, 179: 454–463.

[21] Tian H., Wu M., Shu G., Liu Y., Wang X., Experimental and theoretical study of flammability limits of hydrocarbon-CO_2 mixture. International Journal of Hydrogen Energy, 2017, 42(49): 29597–29605.

[22] Gant S., Pursell M., Lea C., Fletcher J., Rattigan W., Thyer A., Connolly S., Flammability of hydrocarbon and carbon dioxide mixtures. Process Safety and Environmental Protection, 2011, 89: 472–481.

[23] Cao Z., Zhu T., Chemical effects of CO_2 dilution on flame structure and NO formation properties in methane-preheated air counterflow diffusion flame. Journal of Combustion Science and Technology, 2012, 18: 123–130.

[24] Tang C., Huang Z., He J., Jin C., Wang J., Zhang Z., Miao H., Wang X., Measurement of laminar burning velocities and Markstein lengths of propane-air-diluent premixed flames. Transactions of CSICE, 2008, 26: 525–532.

[25] Hu E., Huang Z., Jiang X., Li Q., Zhang X., Kinetic study on laminar burning velocities and ignition delay times of C1-C4 alkanes. Journal of Engineering Thermophysics, 2013, 34: 558–562.

[26] Tang W., He G., Zhou S., Sun W., Cai D., Mei K., The performance and risk assessment of R290 in a 13 kW air source heat pump. Applied Thermal Engineering, 2018, 144: 392–402.

[27] Lemmon E.W., Huber M.L., McLinden M.O., NIST Standard Reference Database 23, Reference Fluid Thermodynamic and Transport Properties (REFPROP), version 9.0. National Institute of Standards and Technology, 2010.

[28] Maaren A. One-step chemical reaction parameters for premixed laminar flames. PhD thesis, Eindhoven University of Technology, 1994.

[29] Wang H., You X., Joshi A., Davis S., Alexander L., Fokion E., Law C., USC mech version II. high-temperature combustion reaction model of H2/CO/C1-C4 compounds. 2007.
Website: http://ignis.usc.edu/USC_Mech_II.htm.

[30] Turanyi T., Applications of sensitivity analysis to combustion chemistry. Reliability engineering & system safety, 1997, 57: 41–48.

[31] Bosschaart K., Goey L., The laminar burning velocity of flames propagating in mixtures of hydrocarbons and air measured with the heat flux method. Combustion and Flame, 2004, 136: 261–269.

[32] Huzayyin A., Moneib H., Shehatta M., Attia A., Laminar burning velocity and explosion index of LPG-air and propane-air mixtures. Fuel, 2008, 87: 39–57.

[33] Tang C., Huang Z., He J., Jin C., Wang X., Miao H., Effects of N_2 dilution on laminar burning characteristics of propane−air premixed flames. Energy & Fuels, 2009, 23: 151–156.

[34] Vagelopoulos C., Egolfopoulos F., Direct experimental determination of laminar flame speeds. Twenty-Seventh Symposium (International) on Combustion, 1998, 27: 513–519.

[35] Yu G., Law C., Wu C., Laminar flame speeds of hydrocarbon + air mixtures with hydrogen addition. Combustion and Flame, 1986, 63: 339–347.

[36] Xie Y., Wang J., Xu N., Yu S., Huang Z., Comparative study on the effect of CO_2 and H_2O dilution on laminar burning characteristics of CO/H_2/air mixtures. International Journal of Hydrogen Energy, 2014, 39: 3450–3458.

[37] Xie Y., Wang J., Zhang M., Gong J., Jin W., Huang Z., Experimental and numerical study on laminar flame characteristics of methane oxy-fuel mixtures highly diluted with CO_2. Energy & Fuels, 2013, 27: 6231–6237.

[38] Qiao L., Kim C., Feath G., Suppression effects of diluents on laminar premixed hydrogen/oxygen/nitrogen flames. Combustion and Flame, 2005, 143: 79–96.

[39] Varghese R.J., Kolekar H., Kumar S., Demarcation of reaction effects on laminar burning velocities of diluted syngas-air mixtures at elevated temperatures. International Journal of Chemical Kinetics, 2019, 51(2): 95–104.